Available online at www.sciencedirect.com
SCIENCE DIRECT
Journal of Molecular Catalysis A: Chemical 243 (2006) 214–220
JOURNAL OF MOLECULAR CATALYSIS A: CHEMICAL
www.elsevier.com/locate/molcata

Chemistry and reactivity of mononuclear manganese oxamate complexes: Oxidative carbon–carbon bond cleavage of *vic*-diols by dioxygen and aldehydes catalyzed by a *trans*-dipyridine manganese(III) complex with a tetradentate *o*-phenylenedioxamate ligand

Santiago Barroso [a], Gonzalo Blay [a], Isabel Fernández [a], José R. Pedro [a,*], Rafael Ruiz-García [a], Emilio Pardo [b], Francesc Lloret [b], M. Carmen Muñoz [c]

[a] *Departament de Química Orgànica, Universitat de València, 46100 Burjassot, València, Spain*
[b] *Departament de Química Inorgànica, Universitat de València, 46100 Burjassot, València, Spain*
[c] *Departamento de Física Aplicada, Universidad Politécnica de València, 46071 València, Spain*

Received 25 May 2005; received in revised form 5 August 2005; accepted 5 August 2005
Available online 26 September 2005

Abstract

Two new mononuclear octahedral manganese(III) complexes with the tetradentate equatorial ligand *o*-phenylenebis(oxamate) (opba) and two aquo (**1a**) or two pyridine (**1b**) axial ligands have been synthesized and characterized structurally, magnetically, and electrochemically. The cyclovoltammogram of **1a** in acetonitrile (25 °C, 0.1 M Bu_4NPF_6) shows an irreversible one-electron oxidation peak at a high anodic potential (E_{ap} = 1.03 V versus SCE), while that of **1b** shows two well-separated one-electron oxidation peaks at moderate to high anodic potentials (E_{ap} = 0.92 and 1.27 V versus SCE), the first redox-wave being quasireversible in nature. The access to formally high-valent Mn^{IV} and Mn^{V} oxidation states for **1b** is attributed to the stabilization effect of axial pyridine ligand coordination. Complex **1b** has been used as an efficient catalyst for the aerobic oxidative cleavage of aromatic *vic*-diols with co-oxidation of pivalaldehyde to pivalic acid. The corresponding aldehydes or ketones are obtained in fair to good yields and moderate selectivities in acetonitrile at 40 °C. Under the same experimental conditions, complex **1a** shows lower efficiencies and selectivities than **1b**. The modulation of catalytic activity by the axial pyridine ligands highlights the role of oxomanganese(V) species as the putative intermediates in these C─C bond cleavage oxidation reactions.

Keywords: Catalysis; C─C bond activation; Manganese; O─O bond activation; Oxidations; Redox properties

1. Introduction

Oxidative carbon–carbon bond cleavage of vicinal diols to carbonyl compounds and carboxylic acids is an important and fairly common reaction in synthetic organic chemistry with implications in other areas of chemistry and biology [1]. This kind of C–C bond breaking reaction is closely related to many important biochemical oxidative processes performed by certain redox enzymes that possess a mononuclear iron-heme prosthetic group with additional cysteine or histidine residues as anchillary axial ligands which serve to modulate their reactivity [2]. These include the side chain cleavage of cholesterol in steroidal hormone biosynthesis catalyzed by cytochrome P450 monooxygenase, and the cleavage of the arylglycerol-β-arylether linkages in the degradation of lignin catalyzed by the heme peroxidase ligninase, which has potential applications in the pulp and paper industry.

Traditionally, the oxidative cleavage of *vic*-diols have been performed with stoichiometric high-valent inorganic oxidants, notably periodic acid [3], sodium bismuthate [4], lead tetraacetate [5], cerium ammonium nitrate [6], manganese dioxide [7] and chromium trioxide [8] reagents. However, these reagents are rather expensive and/or toxic and produce a large amount of waste, which does not conform to the currently urgent demand for a sustainable, green chemistry [9]. From both economic and environmental point of views, alternative catalytic methods that

* Corresponding author. Tel.: +34 963544329; fax: +34 963544328.
E-mail address: jose.r.pedro@uv.es (J.R. Pedro).

1381-1169/$ – see front matter © 2005 Elsevier B.V. All rights reserved.
doi:10.1016/j.molcata.2005.08.027

employ low-cost and readily available catalysts with dioxygen [10], hydrogen peroxide [11] and alkyl hydroperoxides [12] as clean oxidants are then preferable. Among them, those catalytic systems based on the biochemically common, environmentally friendly manganese metal ion in combination with nature's principal oxidants, O_2 and H_2O_2, are particularly appropriate [13].

As a part of our research on the chemistry and the reactivity of manganese complexes with the ligand *o*-phenylenebis(oxamate) (opba) in biomimetic catalytic oxidation reactions of interest in organic synthesis [14], we report herein the first example of a manganese-based catalytic method for the oxidative cleavage of *vic*-diols with dioxygen as oxidant and an aldehyde as reductor. In this contribution, we present a comparative study on the redox and catalytic properties of the two novel mononuclear manganese(III) oxamate complexes $(Me_4N)[Mn(opba)(H_2O)_2]$ (**1a**) and $(Ph_4P)[Mn(opba)(py)_2]\cdot 2H_2O$ (**1b**). The redox-reactivity correlations allow us to ascertain some general molecular aspects of the mechanism of these aerobic oxidation reactions.

2. Experimental

2.1. Materials

All chemicals were of reagent grade quality, and they were purchased from commercial sources and used as received. Non-commercial *vic*-diols were prepared according to literature procedures reported elsewhere. The diethyl ester derivative of the ligand *o*-phenylenebis(oxamic acid) (H_2Et_2opba) was prepared as described earlier [15].

2.2. Preparation

2.2.1. $(Me_4N)[Mn(opba)(H_2O)_2]$ (**1a**)

A solution of H_2Et_2opba (1.54 g, 5.0 mmol) in methanol (50 ml) was charged with a 25% methanol solution of Me_4NOH (8.0 ml, 20.0 mmol). Solid $Mn(CH_3CO_2)_3\cdot 2H_2O$ (1.35 g, 5.0 mmol) was then added in small portions under stirring, and the resulting reaction mixture was further stirred for 15 min at room temperature. A red-brick microcrystalline solid formed abundantly, which was collected by filtration and dried under vacuum. The filtered deep brown solution was reduced to a final volume of 25 ml in a rotatory evaporator. Upon standing at 4 °C in a refrigerator, a second crop separated from the concentrated solution, which was also collected and dried. Yield 60%. Anal. calc. for $C_{14}H_{20}MnN_3O_8$: C, 40.67; H, 10.17; N, 4.84. Found: C, 41.05; H, 9.91; N, 5.12. IR (KBr) ν (cm^{-1}): 1668vs, 1627vs, 1393s and 1279s (CO) from opba. UV–vis (MeCN) λ_{max} (nm): 203 (ε ($M^{-1}\,cm^{-1}$) 26,000), 213 (25,000), 216 (sh) (25,000), 255 (sh) (16,000), 261 (16,000), 308 (sh) (9000), 315 (9000), 415 (sh) (1100), 443 (sh) (700) and 480 (sh) (350).

2.2.2. $(Ph_4P)[Mn(opba)(py)_2]\cdot 2H_2O$ (**1b**)

Complex **1a** (0.83 g, 2.0 mmol) was dissolved in a water–pyridine (4:1) solvent mixture (50 ml). A solution of Ph_4PCl (0.75 g, 2.0 mmol) in acetonitrile (25 ml) was then added to the deep brown solution. Well-shaped golden needles suitable for single crystal X-ray diffraction were deposited from the filtered solution upon standing at room temperature. They were filtered off and air-dried. Yield 80%. Anal. calc. for $C_{44}H_{38}MnN_4O_8P$: C, 63.10; H, 4.54; N, 6.69. Found: C, 63.71; H, 4.35; N, 6.85. IR (KBr) ν (cm^{-1}): 1686vs, 1638vs, 1372s and 1272s (CO) from opba, 1596m, 1474s, and 1439s (CC) from py. UV–vis (MeCN) λ_{max} (nm): 225 (ε ($M^{-1}\,cm^{-1}$) 72,000), 260 (30,000), 275 (25,000), 305 (18,000), 315 (16,000), 420 (sh) (1300), 445 (sh) (900), and 485 (sh) (500).

2.3. Crystal structure determination

Crystal data and structure refinement of **1b**: $C_{44}H_{38}MnN_4O_8P$, $M = 836.68$, monoclinic, space group $P2_1/c$, $a = 15.1723(16)$, $b = 9.9823(16)$, $c = 25.711(2)$ Å, $\beta = 93.268(8)°$, $V = 3887.7(8)$ Å^3, $T = 293(2)$ K, $Z = 4$, $\rho_{calcd} = 1.426\,g\,cm^{-3}$, μ(Mo Kα) = 0.442 mm^{-1}, 5021 unique reflections and 2706 observed with $I > 2\sigma(I)$. Refinement on F^2 of 525 variables with anisotropic thermal parameters for all non-hydrogen atoms gave $R = 0.0733$, $wR = 0.1746$, and $S = 0.962$ (observed data).

2.4. Physical techniques

Elemental analyses (C, H, N) were performed by the Microanalytical Service of the Universidad Autónoma de Madrid (Spain). IR spectra were recorded on a Perkin-Elmer 882 spectrophotometer as KBr pellets. UV–vis solution spectra were recorded at room temperature on a Perkin-Elmer Lambda 2 spectrophotometer. GLC analyses were performed with a Trace GC 2000 (Thermo Quest) using a 30 m × 0.25 mm high-resolution gas chromatography column coated with methylpolysiloxane (5% phenyl). Variable-temperature (2.0–300 K) magnetic susceptibility measurements under an applied magnetic field of 1.0 T were carried out on powdered samples of **1a** and **1b** with a SQUID magnetometer. The experimental magnetic data were corrected for diamagnetism (Pascal's constants), temperature-independent paramagnetism, and the presence of paramagnetic impurities.

Cyclic voltammetry was performed using an EGG M273 PAR scanning potentiostat operating at a scan rate of 10–1000 mV s^{-1}. The electrochemical studies were carried out in acetonitrile using 0.1 M Bu_4NPF_6 as supporting electrolyte and 1.0 mM of **1a** and **1b**. The working electrode was a glassy carbon disk (0.32 cm^2), which was polished with 1.0 μm polishing powder, sonicated, washed with absolute ethanol and acetone, and air-dried. The reference electrode was $AgClO_4$/Ag separated from the test solution by a salt bridge containing the solvent/supporting electrolyte, with platinum as auxiliary electrode. All experiments were performed in standard electrochemical cells at 25 °C under argon. The potential range investigated was from −2.0 to 2.0 V. The formal potentials were measured at a scan rate of 100 mV s^{-1} and were referred to the saturated calomel electrode (SCE), which was consistently measured as −0.26 V versus the $AgClO_4$/Ag electrode. Ferrocene (Fc) was added as internal standard at the end of the measurements, with measured Fc^+/Fc potential of 0.40 V versus SCE.

2.5. Reactivity studies

General procedure for the oxidation of *vic*-diol substrates: reactions were carried out at 40 °C and atmospheric pressure by adding a solution of the substrate (0.26 mmol) in acetonitrile (0.5 ml) to a stirred mixture of the complex (16.0×10^{-3} mmol) in acetonitrile (0.5 ml) under O_2 atmosphere. A solution of pivalaldehyde (1.62 mmol) was added in three equal portions at regular intervals during the course of the reaction, which was monitored by TLC. The reaction mixture was extracted with dichloromethane, washed with saturated aqueous solutions of sodium bicarbonate, and dried with magnesium sulfate. The organic phase was then separated by flash column chromatography on silica gel to obtain the corresponding ketones in pure form, except for acetophenone, which was determined directly by ^{1}H NMR analysis of the reaction mixture using methyl benzilate as internal standard. All ketone products exhibited spectral data consistent with their structures. Alternatively, the yields of aldehydes and carboxylic acids were also determined directly by GLC analysis of the reaction mixture using adamantane as internal standard. Products were identified by comparison of their retention times with those of authentic samples.

3. Results and discussion

3.1. Synthesis

Complex **1a** has been prepared by reaction of Mn^{3+} acetate and the diethyl ester derivative of the ligand H_2Et_2opba, after deprotonation and hydrolysis with Me_4NOH (base/ligand ratio of 4:1) in basic methanol solution, and it was isolated as the tetramethylammonium salt (Scheme 1, left). Complex **1b** has been synthesized from the corresponding diaquo precursor **1a** by treatment with excess pyridine and stoichiometric Ph_4PCl in water–acetonitrile solution, and it was isolated as the tetraphenylphosphonium salt (Scheme 1, right). The chemical identity of **1a** and **1b** has been confirmed by elemental analyses, IR and UV–vis spectroscopies (see Section 2).

3.2. Structure

The structure of **1b** consists of mononuclear manganese(III) complex anions, $[Mn(opba)(py)_2]^-$ (Fig. 1), tetraphenylphosphonium cations, and crystallization water molecules. Selected bond distances and angles are listed in Table 1.

The manganese atom has a tetragonally elongated octahedral coordination geometry typical of a high-spin Mn^{III} ion. The equatorial plane is formed by two amidate nitrogen and two carboxylate oxygen atoms of the tetradentate planar opba ligand, while the axial labile positions are occupied by imine nitrogen atoms from two weakly coordinated *trans* py ligands. The average Mn–N(amidate) and Mn–O(carboxylate) equatorial bond lengths of 1.93 and 1.94 Å, respectively, are close to those of the related dinuclear high-spin manganese(III)-opba complex (average values of 1.91 and 1.96 Å, respectively) [14b]. Yet, the average Mn–N(py) axial bond length of 2.40 Å is larger than the corresponding Mn–O(H_2O) axial bond lengths in the latter complex (average value of 2.30 Å) [14b].

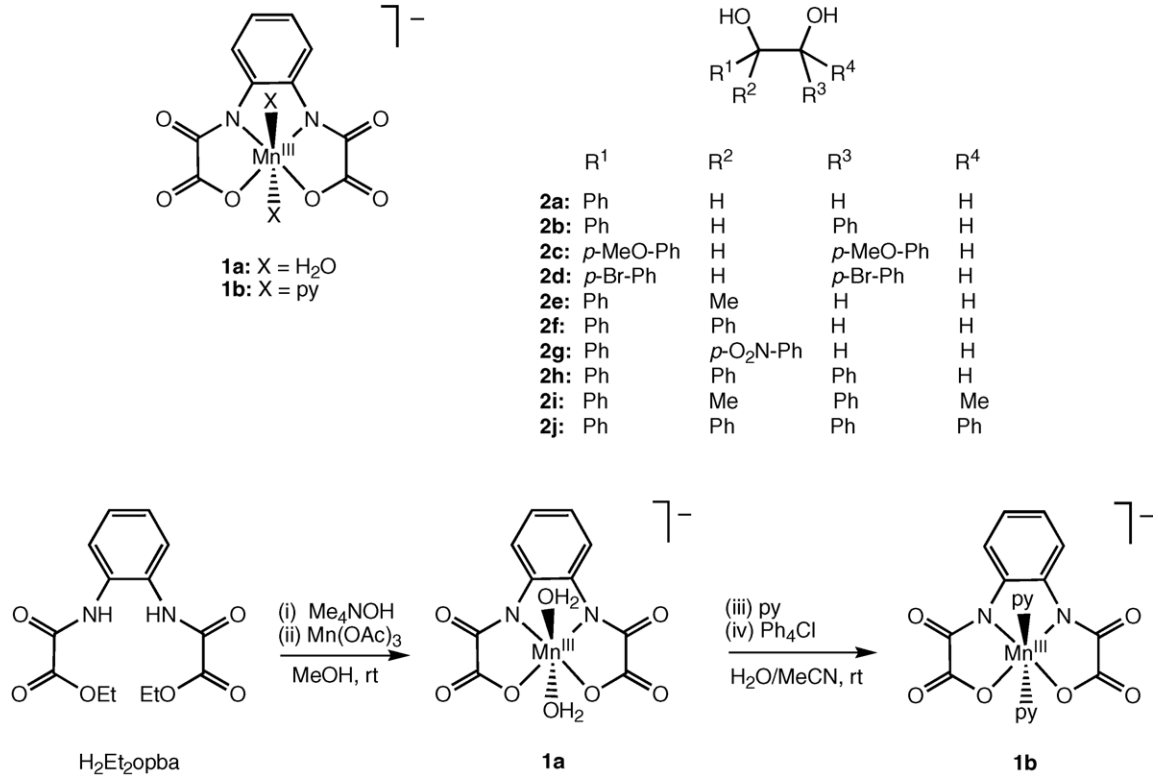

Scheme 1. Synthetic pathway to the manganese-opba complexes.

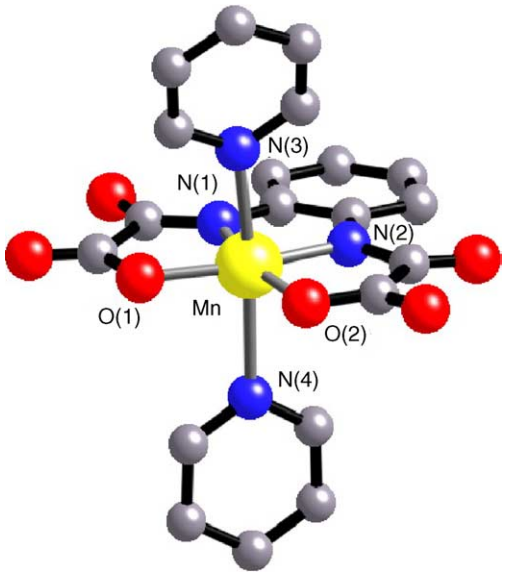

Fig. 1. Perspective view of the anionic mononuclear unit of **1b** with the atom numbering scheme for the first coordination sphere of the metal atom (hydrogen atoms are omitted for clarity).

3.3. Magnetic properties

The variable-temperature magnetic susceptibility data of **1a** and **1b** in the form of $\chi_M T$ versus T plot (χ_M being the molar magnetic susceptibility and T the temperature) are almost identical and consistent with mononuclear six-coordinate octahedral high-spin manganese(III) complexes of axial symmetry (Fig. 2). In the temperature range 50–300 K, the temperature independent $\chi_M T$ value of 3.0 $cm^3\ mol^{-1}$ K (effective magnetic moment of $4.95\mu_B$) is that expected for a high-spin d^4 Mn^{III} ($S = 2$) ion. The abrupt decrease of $\chi_M T$ below 50 K arises from the zero-field splitting (ZFS) of the $S = 2$ Mn^{III} ground state. The least-squares fits of the experimental data through the appropriate spin Hamiltonian ($H = DS_z^2 + g\beta SB$) give axial ZFS parameter (D) values of $-7.4\ cm^{-1}$ for **1a** and $-5.8\ cm^{-1}$ for **1b**, with a common isotropic Zeeman factor (g) value of 2.0 (solid lines in Fig. 2). The D values for **1a** and **1b** are comparable to that reported for the related mononuclear manganese(III)-opbaCl$_2$ complex with two axial dmso ligands [opbaCl$_2$ = *o*-4,5-dichlorophenylenebis(oxamate)] ($D = -4.0\ cm^{-1}$) [16]. The

Table 1
Selected bond distances (Å) and angles (°) for **1b**[a]

Mn—N(1)	1.926(7)	Mn—N(2)	1.926(6)
Mn—O(1)	1.944(6)	Mn—O(2)	1.941(6)
Mn—N(3)	2.373(7)	Mn—N(4)	2.419(8)
N(1)—Mn—N(2)	81.8(3)	N(1)—Mn—O(1)	83.6(3)
N(1)—Mn—O(2)	164.9(3)	N(2)—Mn—O(1)	165.3(3)
N(2)—Mn—O(2)	83.1(3)	O(1)—Mn—O(2)	111.4(3)
N(3)—Mn—N(1)	97.6(3)	N(3)—Mn—N(2)	96.6(3)
N(3)—Mn—O(1)	87.1(3)	N(3)—Mn—O(2)	85.2(3)
N(4)—Mn—N(1)	93.0(3)	N(4)—Mn—N(2)	92.4(3)
N(4)—Mn—O(1)	86.5(3)	N(4)—Mn—O(2)	86.6(3)
N(3)—Mn—N(4)	167.0(2)		

[a] Estimated standard deviations are given in parentheses.

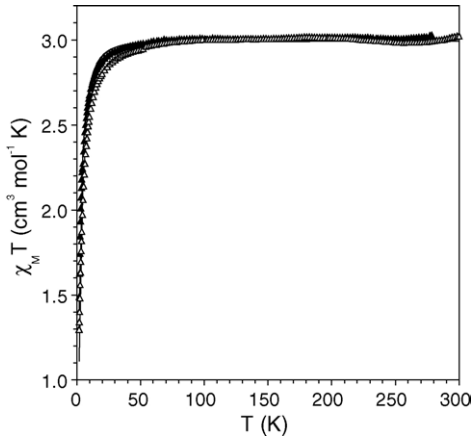

Fig. 2. Temperature dependence of $\chi_M T$ for **1a** (△) and **1b** (▲). Solid lines correspond to the best fits.

moderately large negative axial ZFS for this family of complexes is associated to the important tetragonal elongation of the octahedral metal environment.

3.4. Redox properties

The cyclic voltammetry data of **1a** and **1b** in acetonitrile at 25 °C are drastically different and evidence a significant axial ligand effect on the redox properties. The cyclovoltammogram of **1b** shows two well-separated one-electron oxidation peaks at moderate to high anodic potentials (E_{ap}) of 0.92 and 1.27 V versus SCE (Fig. 3). The first redox oxidation process is quasireversible in nature as revealed by the presence of the corresponding reverse reduction peak at a catodic potential (E_{cp}) of 0.77 V versus SCE (solid line in the inset of Fig. 3). The peak-to-peak separation (ΔE) of 150 mV is, however, larger than that of the Fc^+/Fc couple under the same conditions ($\Delta E = 70$ mV). Contrarily, the cyclovoltammogram of **1a** shows a completely irreversible one-electron oxidation peak at a higher anodic potential

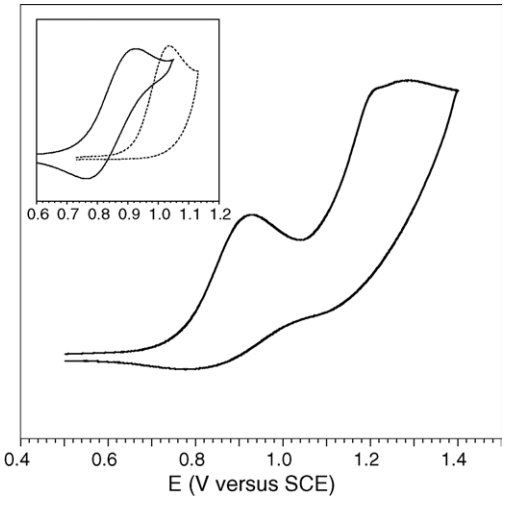

Fig. 3. Cyclovoltammogram of **1b** in MeCN at 25 °C and at scan rate of 100 mV s^{-1}. The inset shows the cyclovoltammogram corresponding to the first redox-wave of **1b** (solid line) compared to that of **1a** (dashed line).

(E_{ap}) of 1.03 V versus SCE (dashed line in the inset of Fig. 3). No reductions are observed for **1a** and **1b** in the potential range studied (up to −2.0 V versus SCE). The differences in the redox behavior of **1a** and **1b** are attributed to the positive effect of axial py ligand coordination on both the thermodinamic and kinetic stabilities of high-valent manganese oxamate complexes, which lowers the oxidation potentials and increases the reversibility of the redox process. Similarly, this indicates that formally Mn^{IV} and Mn^{V} oxidation states are available for the dipyridine adduct of the manganese(III)-opba complex **1b**.

3.5. Reactivity properties

The catalytic activity of **1b** toward the oxidative cleavage of vicinal diols under mild conditions has been examined using some common clean oxidants reported previously, such as dioxygen [10], hydrogen peroxide [11], and *tert*-butyl hydroperoxide [12]. The best results were obtained with O_2 as oxidant in the presence of excess pivalaldehyde as sacrificial reagent in acetonitrile at 40 °C. The results for some representative mono-, di-, tri- and tetra-substituted aromatic *vic*-diols (**2a**–**j**) are summarized in Table 2. Mastrorilli et al. have earlier reported the oxidative cleavage of pinanediols to *cis*-pinonic acids with dioxygen and 2-methylpropanal catalyzed by the cobalt(II)-bis(acetylacetonate) complex [10e]. Yet, to our knowledge, no further extension of the use of this catalytic method based on O_2 plus an aldehyde (the so-called Mukaiyama's catalytic system [17]) for the oxidation of other *vic*-diols has been addressed by the authors.

Complex **1b** catalyzes the oxidation of α-substituted and α,α′-disubstituted diols like phenyl-1,2-ethanediol (**2a**) and 1,2-diphenyl-1,2-ethanediol (**2b**), respectively, to the corresponding aldehyde and carboxylic acid, benzaldehyde and benzoic acid, with good total yields and moderate selectivities (Table 2, entries 2 and 3, respectively). No traces of the corrresponding non-cleaved α-hydroxy- and α-ketoacids, mandelic and phenylglyoxylic acid, are detected for the oxidation of **2a**, whereas only negligible amounts of the corresponding non-cleaved oxidation products, benzoin and benzil, are observed by TLC during the first stages of the oxidation of **2b**. Notably, the total yield of oxidative cleavage products for the oxidation of *para*-substituted 1,2-diphenyl-1,2-ethanediol derivatives (**2b**–**d**) decreases from 65% for **2b** to 61% for **2d**, and to 56% for **2c**, whereas the aldehyde/carboxylic acid ratio increases from 2.6 for **2b** to 3.3 for **2c**, and to 4.5 for **2d**, independently of the electron-donor or electron-acceptor nature of the *para*-substituent (Table 2, entries 3–5). Although the aldehyde/carboxylic acid selectivity values are not exceptional in our catalytic system, this is a considerable improvement compared to that of Mastrorilli et al. using cobalt(II)-bis(acetylacetonate) as catalyst under Mukaiyama's conditions, which lead to carboxylic acids as the majoritary oxidation products [10e].

On the other hand, complex **1b** catalyzes the oxidative cleavage of α,α-disubstituted diols such as 2-phenyl-1,2-propanediol (**2e**), 1,1-diphenyl-1,2-ethanediol (**2f**), and 1-*p*-nitrophenyl-1-phenyl-1,2-ethanediol (**2g**) to the corresponding ketones, acetophenone, benzophenone, and *p*-nitrobenzophenone, respectively, with very good yields (Table 2, entries 7–9). As expected, the oxidation of α,α,α′-trisubstituted diols like triphenyl-1,2-ethanediol (**2h**) affords mixtures of the corresponding ketone and aldehyde, benzophenone and benzaldehyde, respectively, together with the carboxylic acid, benzoic acid, resulting from aldehyde overoxidation (Table 2, entry 10). In the case of α,α,α′,α′-tetrasubstituded diols, the yield of the corresponding ketones depends dramatically on the size of the substituents. Thus, 2,3-diphenyl-2,3-butanediol (**2i**) affords acetophenone with a very good yield of 93% (Table 2, entry 11), while the more sterically-hindered tetraphenyl-1,2-ethanediol (**2j**) gives benzophenone with a very low yield of 10% (Table 2, entry 12).

Finally, we have also examined the catalytic activity of complex **1a**, with aqua in place of pyridine as axial ligands, toward the oxidative cleavage of aromatic *vic*-diols under the same experimental conditions to those used for complex **1b**. Overall, **1a** shows lower efficiencies and selectivities than **1b**. For instance, the yield of ketone for the oxidation of 2-phenyl-1,2-propanediol (**2e**) decreases from 85% with **1b** to 72% with **1a** (Table 2, entry 6), while the aldehyde/carboxylic acid ratio for the oxidation of phenyl-1,2-ethanediol (**2a**) drops from 3.7 with **1b** to 2.2 with **1a** (Table 2, entry 1). A similar effect has been earlier observed for the epoxidation of alkenes with dioxygen and pivalaldehyde catalyzed by the iron(III)-opba complex in the presence of *N*-methylimidazole as exogenous axial ligand [18].

Although the detailed mechanism for the aerobic oxidative cleavage of *vic*-diols catalyzed by complex **1b** still has to be elucidated, some general considerations could be made. First, the marked substrate steric effect on reactivity suggests that free acylperoxy radicals generated in situ from the auto-oxidation of the aldehyde by O_2 are not directly involved as active oxi-

Table 2
Results for the oxidative cleavage of aromatic *vic*-diols with dioxygen and pivalaldehyde[a]

Entry	Complex	Substrate	Time (h)	Products yield (%)[b]		
				Aldehyde	Acid	Ketone
1	**1a**	**2a**	3	33[c]	15[c]	
2	**1b**	**2a**	3	48[c]	13[c]	
3	**1b**	**2b**	3	47[c]	18[c]	
4	**1b**	**2c**	3	43[c]	13[c]	
5	**1b**	**2d**	3	50[c]	11[c]	
6	**1a**	**2e**	6			72[d]
7	**1b**	**2e**	6			85[d]
8	**1b**	**2f**	6			85[e]
9	**1b**	**2g**	6			83[e]
10	**1b**	**2h**	6	55[c]	25[c]	90[c]
11	**1b**	**2i**	6			93[d]
12	**1b**	**2j**	6			10[e,f]

[a] Reactions conditions: see Section 2.
[b] Yields are based on the expected aromatic product for total substrate conversion.
[c] Yields refer to GLC determination.
[d] Yields refer to ^{1}H NMR determination.
[e] Yields refer to isolated and pure oxidation products.
[f] The starting substrate was recovered in 81% yield at the end of the reaction.

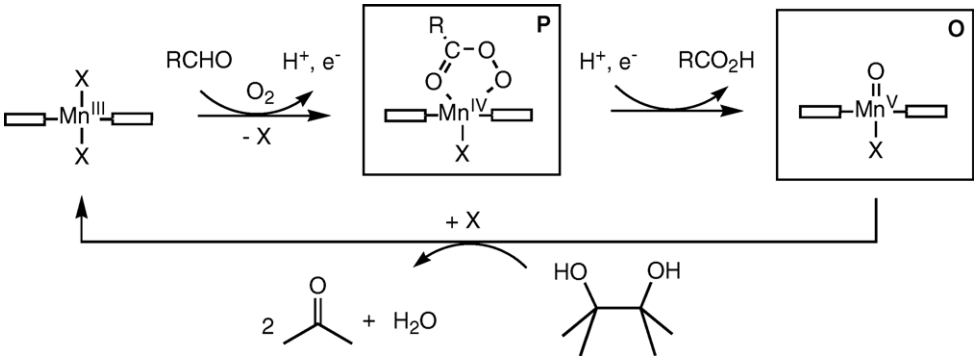

Scheme 2. Proposed mechanistic pathway for the aerobic oxidative cleavage of *vic*-diols with co-oxidation of aldehydes to carboxylic acids catalyzed by the manganese-opba complexes.

dizing agents and bulkier metal-based active oxygen species are likely involved. Second, the axial ligand effect on reactivity suggests that Mn^{V}-oxo species (intermediate **O**), resulting from the pyridine-assisted O–O bond cleavage of the acylperoxide group in the putative Mn^{IV}-acylperoxide species (intermediate **P**), would be the active oxidizing agent (Scheme 2). Interestingly, the three-membered redox catalytic cycle proposed to explain the reported oxidation chemistry is in accordance with the aforementioned redox properties. A similar oxometal reaction pathway has been proposed by Okamoto et al. for the oxidative cleavage of *vic*-diols catalyzed by iron porphyrins with dioxygen as oxidant and dihydropyridine as reductor [10b]. Furthermore, high-valent manganese-oxo complexes of porphyrin [19] and salen-type [20] ligands have been also proposed as reactive intemediates in O-atom transfer oxidation reactions with a variety of terminal oxidants, including O_2 plus an aldehyde [20c,d], in the presence of different exogenous and endogenous axial donor ligands. In this regard, stable terminal oxomanganese(V) complexes with tetradentate alkoxoamidate ligands analogous to that used herein have been prepared by reaction of the corresponding manganese(III) complex with O_2 or $^{t}BuO_2H$ [21].

4. Conclusions

A novel non-heme manganese-based catalytic method for the aerobic oxidative cleavage of a wide range of aromatic *vic*-diols to aldehydes and/or ketones with fair to good yields and moderate selectivities is described. The reaction mechanism involves the reductive dioxygen activation by the new dipyridine-manganese(III) oxamate complex **1b** with pivalaldehyde as reductor, in a manner reminiscent of catalytic oxidation reactions performed by the mononuclear heme iron enzymes cytochrome P450 and ligninase. The results reported herein expand the range of manganese complexes with oxidation resistant ligands capable of activate O_2 or its reduced derivatives, and further confirm the considerable potential of manganese oxamate complexes as robust oxidation catalysts in organic synthesis and biomimetic chemistry. Further mechanistic studies are in progress to determine the exact chemical nature of the active oxidant in these bioinspired green oxidations.

5. Supplementary material

Crystallographic data (excluding structure factors) for **1b** have been deposited with the Cambridge Crystallographic Data Centre, CCDC No. 263906. Copies of the data may be obtained free of charge on application to The Director, CCDC, 12 Union Road, Cambridge CB2 1EZ, UK (fax: +44 1223 336 033; e-mail: deposit@ccdc.cam.ac.uk or www: http://www.ccdc.cam.ac.uk).

Acknowledgements

This work was supported by the Ministerio de Ciencia y Tecnología (Spain) (Project BQU2001–3017) and the Ramón y Cajal program. Further support from the Generalitat Valenciana (Spain) (Project CTIDIA2002–131 and AVCYT Grupos 03/168) is also acknowledged. SB and EP thank the Universitat de València and the Ministerio de Educación, Cultura y Deporte (Spain), respectively, for grants. We are specially thankful to S. Currelli for the assistance with the electrochemical measurements.

References

[1] (a) T.K.M. Shing, in: B.M. Trost, I. Fleming (Eds.), Comprehensive Organic Synthesis, vol. 7, Pergamon Press, Oxford, 1993;
(b) M. Hundlicky, Oxidations in Organic Chemistry, ACS, Washington, 1990.
[2] (a) P.R. Ortiz de Montellano, Cytochrome P450: Structure, Mechanism and Biochemistry, Plenum Press, New York, 1995;
(b) B. Meunier, in: B. Meunier (Ed.), Biomimetic Oxidations Catalyzed by Transition Metal Complexes, Imperial College Press, London, 2000 (Chapter 4).
[3] L.F. Fieser, M. Fieser, Reagents for Organic Synthesis, vol. 1, Wiley, New York, 1967, p. 817.
[4] (a) W. Rigby, J. Chem. Soc. (1950) 1907;
(b) M. Uskokovic, M. Gut, E.N. Trachtenberg, W. Klyne, R.I. Dorfman, J. Am. Chem. Soc. 82 (1960) 4965.
[5] F.J. Wolf, J. Weijjland, Org. Synth., Collect. 4 (1963) 124.
[6] W.S. Trahanovsky, L.H. Young, M.H. Bierman, J. Org. Chem. 34 (1969) 869.
[7] G. Ohloff, W. Giersch, Angew. Chem., Int. Ed. Engl. 12 (1973) 402.
[8] D.F. Tavares, J.P. Borger, Can. J. Chem. 44 (1966) 1323.
[9] (a) Green Chemistry, in: P.T. Anastas, T.C. Williamson (Eds.), Frontiers in Benign Chemical Syntheses and Processes, Oxford University Press, Oxford, 1998;
(b) P.T. Anastas, M.M. Kirchhoff, Acc. Chem. Res. 35 (2002) 686.

[10] (a) T.R. Felthouse, J. Am. Chem. Soc. 109 (1987) 7566;
(b) T. Okamoto, K. Sakai, S. Oka, J. Am. Chem. Soc. 110 (1988) 1187;
(c) T. Iwahama, S. Sakaguchi, Y. Nishiyama, Y. Ishii, Tetrahedron Lett. 36 (1995) 6923;
(d) E. Takezawa, S. Sakaguchi, Y. Ishii, Org. Lett. 1 (1999) 713;
(e) P. Mastrorilli, G.P. Surana, C.F. Nobile, G. Farinola, L. Lopez, J. Mol. Catal. A: Chem. 156 (2000) 279;
(f) G. Du, A. Ellern, L.K. Woo, Inorg. Chem. 43 (2004) 2379.

[11] (a) C. Venturello, M. Ricci, J. Org. Chem. 51 (1986) 1599;
(b) K. Yamakawi, T. Yoshida, H. Nishihara, Y. Ishii, M. Ogawa, Synth. Commun. 16 (1986) 537;
(c) Y. Ishii, K. Yamakawi, T. Ura, H. Yamada, T. Yoshida, M. Ogawa, J. Org. Chem. 53 (1988) 3587;
(d) M. Shimizu, H. Orita, K. Suzuki, T. Hayakawa, S. Hamakawa, K. Takehira, J. Mol. Catal. A: Chem. 114 (1996) 217.

[12] K. Kanada, K. Morimoto, T. Imanaka, Chem. Lett. (1988) 1295.

[13] (a) R. Hage, Recl. Trav. Chim. Pays-Bas 115 (1996) 385;
(b) N.A. Law, M.T. Caudle, V.L. Pecoraro, Adv. Inorg. Chem. 46 (1998) 305.

[14] (a) R. Ruiz, A. Aukauloo, Y. Journaux, I. Fernández, J.R. Pedro, A.L. Roselló, B. Cervera, I. Castro, M.C. Muñoz, Chem. Commun. (1998) 989;
(b) G. Blay, I. Fernández, T. Giménez, J.R. Pedro, R. Ruiz, E. Pardo, F. Lloret, M.C. Muñoz, Chem. Commun. (2001) 2102.

[15] (a) R. Ruiz, C. Surville-Barland, A. Aukauloo, E. Anxolabèhere-Mallart, Y. Journaux, J. Cano, M.C. Muñoz, J. Chem. Soc., Dalton Trans. (1997) 745;
(b) B. Cervera, J.L. Sanz, M.J. Ibáñez, G. Vila, F. Lloret, M. Julve, R. Ruiz, X. Ottenwaelder, A. Aukauloo, S. Poussereau, Y. Journaux, M.C. Muñoz, J. Chem. Soc., Dalton Trans. (1998) 781.

[16] M. Fettouhi, L. Ouahab, A. Boukhari, O. Cador, C. Mathonière, O. Kahn, Inorg. Chem. 35 (1996) 4932.

[17] (a) T. Mukaiyama, Bull. Chem. Soc. Jpn. 68 (1995) 17;
(b) T. Mukaiyama, Aldrichim. Acta 29 (1996) 59.

[18] R. Ruiz, M. Traianidis, A. Aukauloo, Y. Journaux, I. Fernández, J.R. Pedro, B. Cervera, I. Castro, M.C. Muñoz, Chem. Commun. (1997) 2283.

[19] (a) S. Banfi, F. Montanari, G. Pozzi, S. Quici, Gazz. Chim. Ital. 123 (1993) 617;
(b) P.L. Anelli, S. Banfi, F. Legramandi, F. Montanari, G. Pozzi, S. Quici, J. Chem. Soc., Perkin Trans. (1993) 1345.

[20] (a) T. Schwenkreis, A. Berkessel, Tetrahedron Lett. 34 (1993) 4785;
(b) P. Pietikäinen, Tetrahedron Lett. 35 (1994) 941;
(c) K. Imagawa, T. Nagata, T. Yamada, T. Mukaiyama, Chem. Lett. (1994) 527;
(d) T. Nagata, K. Imagawa, T. Yamada, T. Mukaiyama, Bull. Chem. Soc. Jpn. 67 (1994) 2248;
(e) N.S. Finney, P.J. Pospisil, S. Chang, M. Palucki, R.G. Konsler, K.B. Hansen, E.N. Jacobsen, Angew. Chem., Int. Ed. Engl. 36 (1997) 1720.

[21] (a) F.M. McDonnell, N.L.P. Fackler, C. Stern, T.V. O'Halloran, J. Am. Chem. Soc. 116 (1994) 7431;
(b) T.J. Collins, S.W. Gordon-Wylie, J. Am. Chem. Soc. 111 (1989) 4511.